



Research paper

Nucleation and growth rate determination on alkali-activated slag under various sodium hydroxide molarity

**Rosnita Mohamed¹, Rafiza Abd Razak²,
Mohd Mustafa Al Bakri Abdullah³, Shayfull Zamree Abd Rahim⁴,
Nurul Aida Mohd Mortar⁵, Liyana Jamaludin⁶, Marcin Nabialek⁷**

Abstract: Alkali-activated slag has been noted as one of potential alternatives to the ordinary Portland cement due to its properties including high early strength performance and capability of ambient curing. However, there is still limited studies available on elucidating the reaction processes towards producing the excellent properties. This study aims to elucidate the mechanism of alkali activation of slag under different molarities of sodium hydroxide, which is one of the most influential factors on the properties of alkali-activated slag. Heat evolution of alkali-activated slag was used as a real-time monitoring technique. For mix designation, the molarity of sodium hydroxide was varied from 6 M to 14 M, with solid-to-liquid

¹MSc., Faculty of Chemical Engineering and Technology, University of Malaysia Perlis (UniMAP), Perlis, Malaysia; Geopolymer and Green Technology, Centre of Excellence (CEGeoGTech), University of Malaysia Perlis (UniMAP), Perlis, Malaysia, e-mail: rosnitamohamed21@gmail.com, ORCID: 0000-0002-7154-2216

²Associate Prof., PhD., Eng., Faculty of Civil Engineering and Technology, University of Malaysia Perlis (UniMAP), Perlis, Malaysia; Geopolymer and Green Technology, Centre of Excellence (CEGeoGTech), University of Malaysia Perlis (UniMAP), Perlis, Malaysia, e-mail: rafizarazak@unimap.edu.my, ORCID: 0000-0001-5499-8564

³Prof., PhD., Eng., Faculty of Chemical Engineering and Technology, University of Malaysia Perlis (UniMAP), Perlis, Malaysia; Geopolymer and Green Technology, Centre of Excellence (CEGeoGTech), University of Malaysia Perlis (UniMAP), Perlis, Malaysia, e-mail: mustafa_albakri@unimap.edu.my, ORCID: 0000-0002-9779-8586

⁴Associate Prof., PhD., Eng., Faculty of Mechanical Engineering and Technology, University Malaysia Perlis (UniMAP), Perlis, Malaysia; Geopolymer and Green Technology, Centre of Excellence (CEGeoGTech), University of Malaysia Perlis (UniMAP), Perlis, Malaysia, e-mail: shayfull@unimap.edu.my, ORCID: 0000-0002-1458-9157

⁵MSc., Eng., Faculty of Chemical Engineering and Technology, University of Malaysia Perlis (UniMAP), Perlis, Malaysia; Geopolymer and Green Technology, Centre of Excellence (CEGeoGTech), University of Malaysia Perlis (UniMAP), Perlis, Malaysia, e-mail: nurulaida@unimap.edu.my, ORCID: 0000-0001-5668-3080

⁶MSc., Eng., Faculty of Mechanical Engineering and Technology, University of Malaysia Perlis (UniMAP), Perlis, Malaysia; Geopolymer and Green Technology, Centre of Excellence (CEGeoGTech), University of Malaysia Perlis (UniMAP), Perlis, Malaysia, e-mail: liyanajamaludin@unimap.edu.my, ORCID: 0000-0001-6984-6512

⁷Prof., PhD., Department of Physics, Faculty of Production Engineering and Materials Technology, Czestochowa University of Technology, al. ArmiiKrajowej 19, 42-200 Czestochowa, Poland, e-mail: nmarcell@wp.pl, ORCID: 0000-0001-6585-3918

ratios of 0.6 and alkali activator ratios of 2.0 remaining constant. The calorimetric data obtained was further used for determination of degree of reaction, nucleation and growth rate mechanism using Johnson–Mehl Avrami Kolmogorov model. According to the findings, it was found that regardless of various molarity of sodium hydroxide applied, the nucleation mechanism and growth is governed by instantaneous heterogeneous nucleation with rod-like growth as the n value is approaching 1 in which is observed from the morphology of the alkali-activated slag at lowest molarity applied (6 M). Furthermore, increasing in molarity of sodium hydroxide was found to decrease the total heat evolved and the lowest was obtained when using 14 M.

Keywords: alkali-activated slag, heat evolution, Johnson–Mehl Avrami Kolmogorov model, molarity of sodium hydroxide, and nucleation and growth rate

1. Introduction

Alkali-activated slag has been introduced in alkali-activated materials (AAMs) research as one of promising materials as alternative to the Portland cement (OPC). There are different types of slag depending on the manufacturing wastes including ground granulated blast furnace slag (GGBFS) [1], coal-gangue slag [2] and magnesia-ferriferous slag [3]. GGBFS has been widely used in the construction industry as an additive to improve the properties of mortar and concrete. It is widely accepted that the use of GGBFS can improve the properties of the binder produced, particularly its strength performance during the early stages of development [4]. Furthermore, GGBFS has a chemical composition that closely resembles that of OPC. As a result, GGBFS has been identified as a promising aluminosilicate material for the production of alkali-activated materials that possess similar properties to OPC. Therefore, researches on evaluating the alkali-activated slag derived from GGBFS has been widely carried out in alkali-activated materials field. However, there is still lack of information available on the insight mechanism of alkali activation of AAS that led to the comparable properties reported where most of the studies emphasized the addition effect of GGBFS on improving the AAMs produced. For this purpose, a real-time technique is necessary for monitoring the reaction process occurred during alkali activation process. There have been numerous real-time techniques introduced for monitoring the alkali activation process. These techniques include monitoring on the relative humidity evolution by Hu et al. [5], structural and chemical bonding evolution by Liu et al. [6] and ultrasonic evolution Cao et al. [7] and Li et al. [8]. Apart from these methods of monitoring, heat evolution in which is widely used for monitoring OPC hydration is also denoted as a reliable method for monitoring the reaction process occurred during alkali activation of AAMs.

In heat evolution, The significant changes occurred throughout alkali activation process will be detected in term of heat flow thus led to formation of several peaks on the calorimetric

data. The calorimetric data obtained can be further used for elucidation of reaction kinetics on alkali activation process including activation energy, nucleation mechanism and growth rate. In addition, it is well known that the changes in reaction rate during alkali activation are primarily influenced by the variation in influence factors, such as solid precursors used for alkali activation, molarity of alkali solution used, solid-to-liquid ratios, alkali activator ratio, and curing temperature.

The effect of curing temperature on the heat evolution of alkali-activated materials, including geopolymer, where the reaction kinetics were visibly notable with increasing temperature application has been extensively reported included by Nath et al. [9], and Zhang et al. [10]. Due to the fact that it is already known that additional heat enhances the reaction process, it has been difficult to evaluate the effect of other influence factors applied during the reaction process, necessitating additional research for the ambient temperature. In addition to the curing temperature, the molarity of the alkali solution is known to play a significant role during the dissolution of solid precursors. It is believed that increasing the alkalinity improves the dissolution rates for the formation of AAS monomers significantly. In AAMs research, sodium hydroxide (NaOH) is typically employed as a liquid precursor for the alkali activation process, and is typically combined with sodium silicate (Na_2SiO_3). Increasing in molarity of NaOH increases the hydroxide ions (OH^-) which is crucial for dissolution with more silicon and aluminum ions dissolving due to the weaker strengths of Si-O and Al-O bonds in the alkaline environment.

Therefore, this study intends to observe the effect of varying molarity of sodium hydroxide from 6 M until 14 M on alkali activation of slag using ground granulated blast furnace slag as solid precursor via heat evolution. Moreover, since there are still limited studies available on utilizing the Johnson Mehl Avrami Kolmogorov model (JMAK) for evaluating the insight mechanism of alkali activation process, this study will use JMAK model for elucidation on the nucleation and growth rate mechanism of alkali activation of slag. JMAK model has been established for a very long time in which helps to define and explain the allotropic phase change in solidification where the nucleation and growth processes are the foundation of the model thus making it reliable for specification on the nucleation and growth of alkali activation process. This model have been applied in many applications including crystallization explanation of polymers [11], crystal dissolution kinetics [12], crystallization of metallic glasses [13] and reaction kinetics of geopolymerization [14]. The general equation for Avrami's Theory is written as in Eq. (1.1) [15].

$$(1.1) \quad \ln[-\ln(1 - X_c)] = \ln k + n \ln t$$

where X_c or sometimes denoted as X_t is degree of crystallinity, n , is the phenomenological index of crystallization, which can be used to discern between different mechanisms of crystallization and k represents crystallization kinetic constant (growth rate) for nucleation and growth. Thus, from this model, the nucleation and growth mechanism of alkali activation of slag with different molarity of NaOH will be determined in this study using the calorimetric data from the heat evolution. In addition, the morphology of AAS will be observed at 1 day of age in order to monitor the development of AAS during nucleation and growth.

2. Methodology

2.1. Materials and mixing design

In this work, ground granulated blast furnace slag (GGBFS) which was supplied by Macro Dimension Concrete, MDC at Chuping Plant was used as a solid precursor for the formation of alkali-activated materials and will be referred to as slag throughout, as no other slag was employed. The characterization for slag was carried out including chemical composition and morphology. The chemical composition of slag was determined using X-Ray fluorescence (XRF) and the morphology of the slag particles was observed by using scanning electron microscope (SEM) with magnification of 5000 \times . According to the XRF result obtained, in term of percentage of weight, it was found that the slag used in this study is mainly composed of 54.20% of calcium oxide (CaO), followed by 25.60% of silicon dioxide (SiO₂) and 10.90% of aluminum oxide (Al₂O₃). Furthermore, the slag used in this work also contains 0.76% iron oxide (Fe₂O₃), 3.10% magnesium oxide (MgO), 1.52% titanium dioxide (TiO₂), and 1.95% sulphur trioxide (SO₃), with the majority of them being less than 5% composition. Meanwhile as depicted by Fig. 1, it was observed that the slag particles were irregular in shapes with sharp edge, where the surface area availability of the nucleation site will be different for each of the particles.

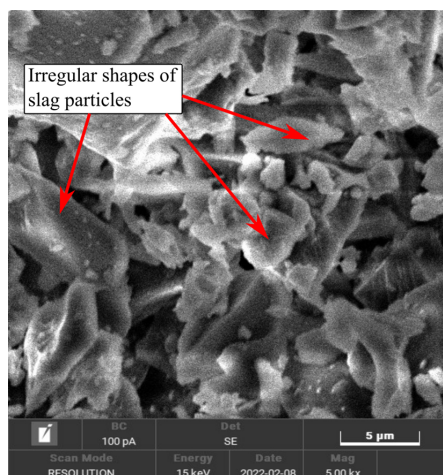


Fig. 1. Morphology of slag particles used in this study

For liquid precursors, a combination of sodium hydroxide (NaOH) and sodium silicate was utilized. Prior mixing of these two, the pellet-form NaOH of 97% purity had to be diluted to the desired molarity to be applied. Meanwhile, the employed Na₂SiO₃ was already in solution form. The details of mixing designation for this study can be summarized as in Table 1. Alkali-activated slag (denoted as AAS throughout this study) was synthesized by mixing both of solid and liquid precursors at a fixed mixing time (within five minutes) for each of the ratios applied. Once mixing was done, the sample was directly used for determination of heat evolution.

Table 1. Mixing Design and process

Solid-to-liquid ratio	Alkali activator ratio	Molarity of NaOH
0.6	2.0	6 M
0.6	2.0	8 M
0.6	2.0	10 M
0.6	2.0	12 M
0.6	2.0	14 M

3. Testing procedure

3.1. Determination of heat evolution

A heat flow calorimeter supplied by “ToniCAL, Toni Technik” was used to measure the heat evolution of alkali-activated slag (AAS) under isothermal conditions at a temperature of 26°C. The test was conducted as per description of ASTM C1679-14 [16] and ASTM C1702 [17]. External mixing was applied in this study and mixing procedure was conducted for a duration of five minutes for each of the mix designation in order to standardize the mixing time, considering the sensitivity of the properties of AAS. The heat evolution was monitored for 72 hours, equivalent to the duration of time used by previous researchers to monitor the heat of OPC hydration. The collected data were interpreted as the rate of heat evolution (dQ/dt in J/gh) and the total cumulative amount of heat evolved ($Q(t)$ in J/g).

3.2. Determination of degree of reaction

The degree of the reaction, α was determined by using Schutter method [18] by using the following Eq. (3.1).

$$(3.1) \quad \frac{Q(t)}{Q_{\max}}$$

where $Q(t)$ is the cumulative heat evolved at time t , and Q_{\max} is the total or the maximum heat evolved to complete the reaction. Q_{\max} can be obtained from experimental data of calorimetry.

3.3. Determination of nucleation mechanism

The Johnson–Mehl–Avrami–Kolmogorov (JMAK) Model, also known as Avrami’s theory, was used to determine the nucleation and growth process of AAS. The JMAK’s exponent (n) and k (growth rate) can be calculated using Eq. (3.1). Since, the degree of reaction, α was calculated, the X_c in the equation which represent rate of crystallinity was replaced with α thus the equation would be written as in Eq. (3.2).

$$(3.2) \quad \ln [-\ln(1 - \alpha)] = \ln k + n \ln t$$

Equation (3.2) was used to plot a linear graph of $y = mx + c$, where $y = \ln[-\ln(1 - \alpha)]$, $x = \ln t$. The slope of the straight line represents the JMAK's exponent (n) and the y -intercept of the straight-line (c) yields JMAK's growth rate, k . The value of n enables us to quantify the crystallization behaviour of the alkali-activated slag during heat evolution.

3.4. Morphology characterization of alkali-activated slag

Surface morphology of alkali-activated slag pastes was observed by using Scanning Electron Microscope JSM-6460LA model (JEOL). The magnification required was up to 5000 \times magnification in order to observe possible nucleation development occurred. A cross-sectioned sample was required in order to observe the surface morphology of the AAS and the sample was required to coat with palladium (Pd) prior testing.

4. Results and Discussions

4.1. Heat evolution analysis

The heat evolution of alkali-activated slag (AAS) with different molarity of sodium hydroxide is depicted as in Fig. 2(a). The total cumulative heat evolved determined from the calorimetric data was also illustrated as in Fig. 2(b).

From Fig. 2, it was found that there is only one notable peak observed for all molarity applied. Generally, increasing in molarity led to significant changes to the appearance of the peak. Increasing in molarity of sodium hydroxide (NaOH) from 6 M to 10 M led to increase in intensity of the peak and the highest was at 10 M (99.15 J/gh). This is in line with past researches that claimed increasing in molarity of NaOH causes increasing in heat flow due to the rapid reaction process in which is usually denoted as wetting and dissolution of alkali activation [19, 20]. However, it is believed that the reaction processes during alkali activation occurred simultaneously. Therefore, alongside with wetting, dissolution process which led to the formation of monomers of AAS will directly undergo nucleation and polymerization to form AAS gels. Increasing in OH^- ions led to more monomer's formation including $[\text{SiO}_4]^-$, $[\text{SiO}_4]^{2-}$, $[\text{AlO}_4]^-$ for alkali activation processes. Since the reaction processes occurred during hydration and alkali activation are generally overlapped, therefore it was found that the total cumulative heat evolved increased with increasing molarity of sodium hydroxide from 6 M (346.92 J/g) to 10 M (370.97 J/g) which suggesting the rapid reaction with increasing molarity. In addition, the high chemical composition of calcium in the AAS system is believed to contribute to hardening process of alkali-activated slag with the rapid hydration process occurred with increasing hydroxide ions thus causing the increasing total cumulative heat evolved.

However, further increases in molarity for 12 M and 14 M were found to reduce the heat flow of alkali-activated slag, with the maximum intensity peak observed at 14 M (41.41 J/gh) being the lowest in comparison to the maximum peak intensity for other molarity of NaOH applied. In addition, the 12 M and 14 M peak formations are broader than those of 6 M, 8 M, and 10 M. With an increase in the availability of OH^- ions in the alkali-activated slag system,

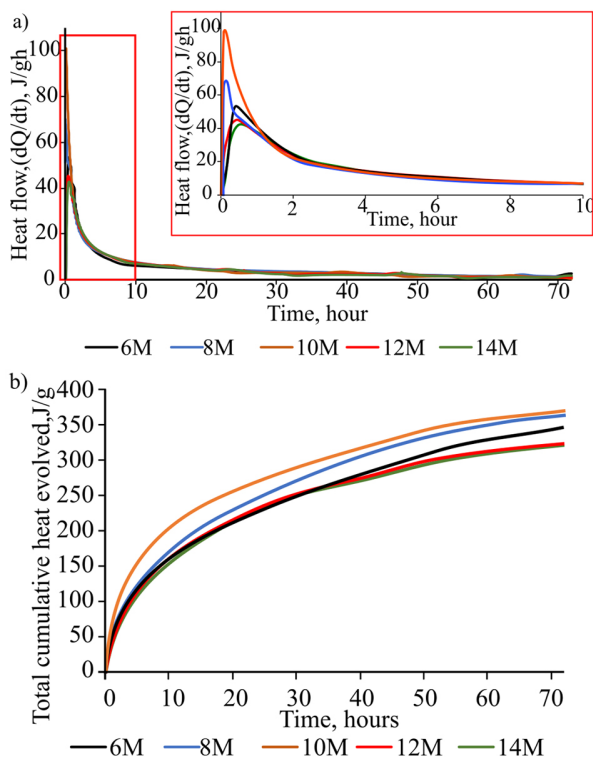


Fig. 2. Heat evolution and total cumulative heat evolved of alkali-activated slag

more monomers formed, leading to an increase in hydration and polymerization, which in turn led to the formation of more AAS gels, thus hindering the heat flow in the system. This accounted for the broad development of the 12 M and 14 M peaks and slightly shift to the right. Similar observation was found for the total cumulative heat evolved, where the total cumulative heat evolved started to reduce at 12 M and 14 M (324 J/g and 320 J/g respectively) in which confirmed the hindering with increasing in formation of AAS gels.

4.2. Degree of reaction analysis

The Schutter equation was used to compute the degree of reaction of alkali activation slag with different molarities of sodium hydroxide used in this investigation, and the results are illustrated in Fig. 3. Due to the fact that small increment of molarity (2M) was applied in this study, the pattern for the reaction was essentially identical to each other.

Within 10 hours of the reaction process, increasing the molarity up to 10 M was found to cause a rapid degree of reaction, with the greatest degree of reaction at 10 M (0.58) and the least degree of reaction at 6 M (0.42). Another significant finding was that, despite the low heat flow during the first 10 hours of the reaction, the degree of reaction for molarities of 12 M and 14 M

was still higher than 6 M (0.48 and 0.55, respectively). This occurrence proved that increasing the molarity of sodium hydroxide leads to increase the reaction rate, especially during the early reaction phases of alkali activation, which comprise wetting, dissolution, and hydration.

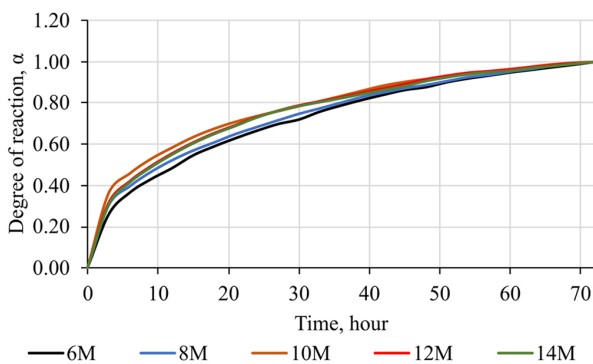


Fig. 3. Degree of reaction analysis of alkali-activated slag

Furthermore, the high calcium content in the slag particles can be corresponding to the rapid increase in reaction degree. Calcium hydration contributes significantly to the hardening of AAS, resulting in calcium hydrated products such as calcium silicate hydrates (CSH) and calcium aluminate silicate hydrates (CASH) [4]. The increase in degree of reaction rate followed a similar trend until 40 hours into the reaction process. However, after 40 hours of reaction, the degree of reaction began to be almost same in reaction rate regardless of molarity applied, implying that minimal heat evolved during this period. This occurrence also shown that the heat evolved mostly during the early stages of the reaction (0–40 hours).

4.3. Nucleation and growth mechanism analysis

The degree of reaction determined were applied for further analysis on nucleation and growth mechanism of alkali-activated slag (AAS) with different molarity of NaOH applied using Johnson–Mehl Avrami Kolmogorov model. Eq. (3.2) was used and the plot for JMAK with different molarity of sodium hydroxide was depicted as in Fig. 4. The slope of the plot represents the n value (JMAK exponent) and the intercept of the plot represent $\ln k$ (growth rate) of the alkali activation process. The extraction from the plot can be summarized as in Table 2.

Based on Fig. 4 and Table 2, the values of n that represent the JMAK exponent range between 0.8348 and 0.8992, whereas the values of k that were calculated from the intercept of the graphs range between 0.0779 and 0.1043. From the n values which are more than 0.5 and approaching $n = 1$, it can be deduced that the nucleation growth mechanism of AAS is same regardless of different molarity of sodium hydroxide applied. In addition, as the n values is approaching 1, it can be surmised that the nucleation mechanism of alkali activation of slag in this study is governed by instantaneous nucleation mechanism (one dimensional) with a rod-like growth or sometimes denoted as needle-like growth. In term of the n values which is less than 1 obtained, it can be attributed to a decrease in the growth rate of radial

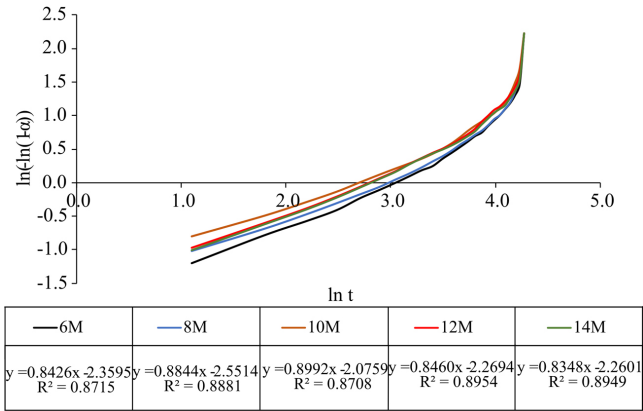


Fig. 4. Johnson–Mehl Avrami Kolmogorov plot of alkali-activated slag

Table 2. Extraction from JMAK Model of AAS with different molarity of sodium hydroxide applied

Molarity of sodium hydroxide	Avrami exponent (n)	Growth rate (k) min ⁻¹
6	0.8426	0.0914
8	0.8844	0.0779
10	0.8992	0.1254
12	0.8460	0.1034
14	0.8348	0.1043

nuclei as a result of the inhibition of previously formed nuclei and a decrease in molecular mobility [14]. Meanwhile, contradict to *n* value, growth rate (*k*) is inversely proportional to *n* value. The increasing values of *k* which represent the growth rate of the alkali activation, it concluded that increasing in molarity of sodium hydroxide led to increasing growth rate with more availability of OH⁻ ions for dissolution process thus forming more monomers for nucleation and polymerization.

4.4. Morphology analysis

Morphology analysis was performed to observe the development of the alkali-activated slag (AAS), particularly the nucleation growth as the molarity of sodium hydroxide (NaOH) applied increased. The morphology was observed at 1 day of age, which is after the period of accelerated degree of reaction and depicted as in Fig. 5.

Fig. 5 reveals that the densification of AAS is positively correlated with increasing NaOH concentration. In this study, alkali-activated slag with 14 M had the densest morphology compared to 6 M, 8 M, 10 M, and 12 M, all of which contained voids within their morphologies.

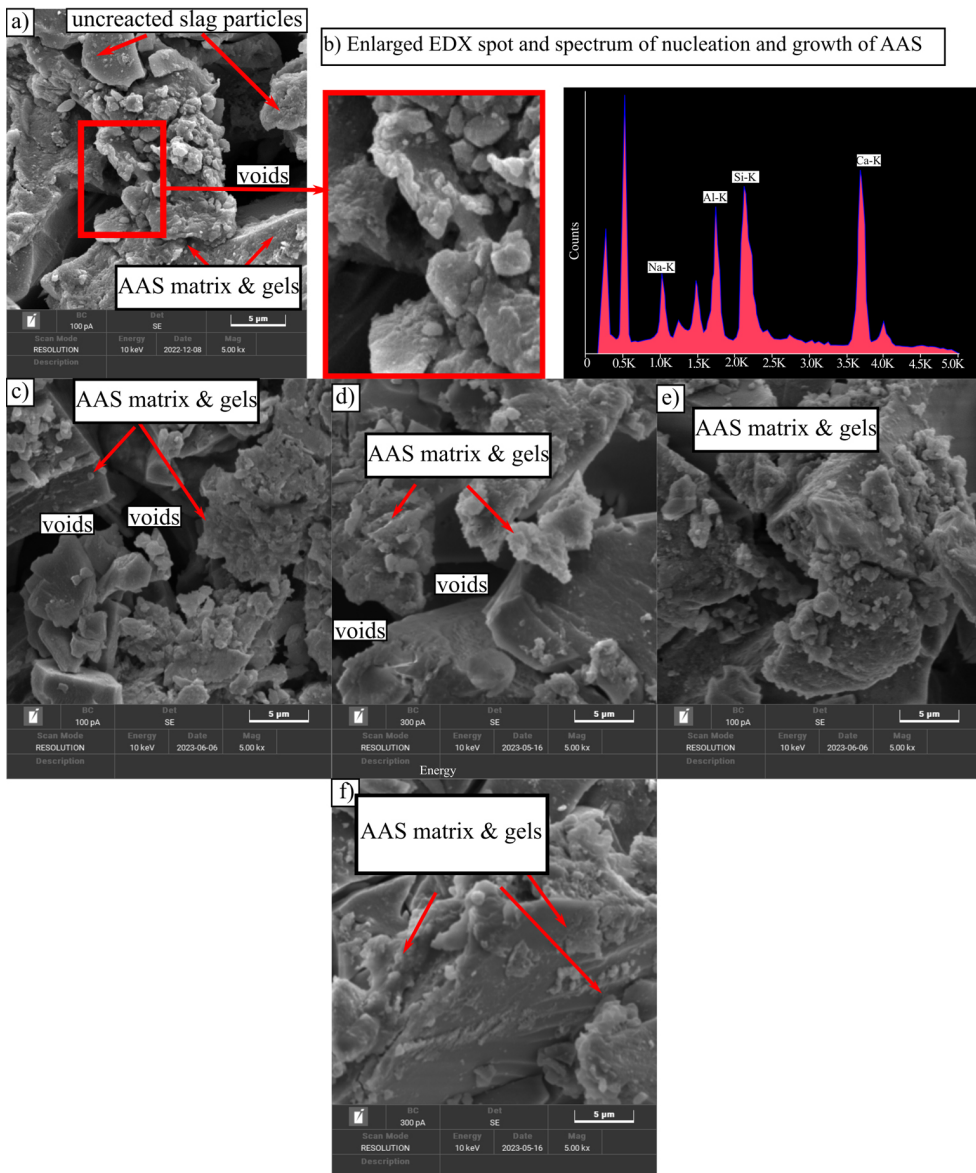


Fig. 5. Morphology of 1-day age alkali activated slag; a) 6 M, b) Enlarged EDX spot and spectrum of nucleation and growth of AAS, c) 8 M, d) 10 M, e) 12 M and f) 14 M

This observation proved that the reduction in total cumulative heat evolved for 12 M and 14 M was due to the hindering by the alkali-activated matrix and gels densification. In addition, the nucleation development of the alkali-activated slag polymeric matrix consisting of Si-O-T (T: Si, Al, Na, Ca) bonds was observed when 6 M molarity was used. The development of

nucleation growth was discovered to be consistent with the growth dimensionality proposed by the JMAK model, which predicted that nucleation growth would occur instantaneously in rod-like growth. In addition, Energy Dispersive X-ray (EDX) microanalysis was conducted to ascertain the chemical composition of the observed nucleation growth. According to the intensity of the peak counts of Si Al and Ca, it is possible to conclude that the observed nucleation consisted of CASH, CSH, and NASH gels, which are the products of alkali activation.

5. Conclusions

In a nutshell, determination of heat evolution can be noted as significant indicator for understanding the alkali activation process of alkali-activated slag. From the real-time monitoring, it was found that increasing in molarity of sodium hydroxide (NaOH) generally increases the total cumulative heat evolved alongside with increasing the maximum intensity of the heat evolution peak. However, it was discovered that further increase in molarity decreases both the total cumulative heat evolved and the maximum intensity of the heat evolution peak, as a result of the densification of the alkali-activated slag system caused by the rapid reaction, thereby hindering the heat flow in the system. The densification of the polymeric gels was proven by the morphology observed specifically at 12 M and 14 M. On top of that, the nucleation and growth mechanism analysis that was elucidated by using the calorimetric data of heat evolution and the Johnson Mehl Avrami Kolmogrov model revealed that, regardless of the difference in molarity of sodium hydroxide used, the nucleation mechanism of alkali activation of slag was governed by an instantaneous nucleation mechanism (one dimensional) with a rod-like growth or sometimes referred to as needle-like growth as the JMAK exponent (n values) obtained is approaching 1.

In the meantime, the growth rate extracted from the JMAK plot proved that increasing the molarity of sodium hydroxide significantly raised the growth rate of reaction during the first 10 hours of the reaction process, as indicated by the degree of reaction results obtained. The findings obtained from this work are considered significant for elucidating the effect of the molarity of sodium hydroxide on the reaction process of alkali activation. This is due to the fact that the molarity of the alkali solution used is one of the crucial influence factors to be concerned with in terms of producing alkali-activated materials with superior properties according to the desired applications. In addition, due to the various properties including physical and mechanical properties reported by past researches, this work is worthwhile to be further explored in order for better understanding on how the other influence factors such as the effect of different aluminosilicate precursors utilized, the effect of different solid-to-liquid ratios, and the effect of the alkali activator ratio used when dealing with the combination of sodium silicate (Na_2SiO_3) and sodium hydroxide as alkali activator affecting the alkali-activated materials in term of its reaction process. It is expected that each of these influence factors will affect the chemical composition of the alkali-activated materials system, thus leading to variations in heat evolution.

Acknowledgements

The authors acknowledge Geopolymer & Green Technology, Centre of Excellence (CE-GeoGTech), University of Malaysia Perlis (UniMAP), Perlis, Malaysia, School of Civil Engineering, College of Engineering, University of MARA Technology (UiTM) Shah Alam, and Faculty of Chemical Engineering Technology, University of Malaysia Perlis for the lab facilities. Special thanks to those who contributed to this project directly or indirectly.

References

- [1] A.H. Mahmood, M. Babae, S.J. Foster, and A. Castel, "Capturing the early-age physicochemical transformations of alkali-activated fly ash and slag using ultrasonic pulse velocity technique", *Cement and Concrete Composites*, vol. 130, art. no. 104529, 2022, doi: [10.1016/j.cemconcomp.2022.104529](https://doi.org/10.1016/j.cemconcomp.2022.104529).
- [2] H. Ma, et al., "Preparation and reaction mechanism characterization of alkali-activated coal gangue-slag materials", *Materials (Basel)*, vol. 12, no. 14, 2019, doi: [10.3390/ma12142250](https://doi.org/10.3390/ma12142250).
- [3] A.M. Kalinkin, B.I. Gurevich, M.S. Myshenkov, E.V. Kalinkina, and I.A. Zvereva, "A calorimetric study of hydration of magnesia-ferriferous slag mechanically activated in air and in CO₂ atmosphere", *Journal of Thermal Analysis and Calorimetry*, vol. 134, no. 1, pp. 165–171, 2018, doi: [10.1007/s10973-018-7439-9](https://doi.org/10.1007/s10973-018-7439-9).
- [4] V.C. Prabha and V. Revathi, "Geopolymer Mortar Incorporating High Calcium Fly Ash and Silica Fume", *Archives of Civil Engineering*, vol. 65, no. 1, pp. 3–16, 2019, doi: [10.2478/ace-2019-0001](https://doi.org/10.2478/ace-2019-0001).
- [5] Z. Hu, M. Wyrzykowski, and P. Lura, "Estimation of reaction kinetics of geopolymers at early ages", *Cement and Concrete Research*, vol. 129, art. no. 105971, 2020, doi: [10.1016/j.cemconres.2020.105971](https://doi.org/10.1016/j.cemconres.2020.105971).
- [6] B. Liu, K. Zhuang, D. Li, Y. Fang, and G. Pan, "Understanding the early reaction and structural evolution of alkali activated slag optimized using K-A-S-H nanoparticles with varying K₂O/SiO₂ ratios", *Composites Part B: Engineering*, vol. 200, art. no. 108311, 2020, doi: [10.1016/j.compositesb.2020.108311](https://doi.org/10.1016/j.compositesb.2020.108311).
- [7] R. Cao, S. Zhang, N. Banthia, Y. Zhang, and Z. Zhang, "Interpreting the early-age reaction process of alkali-activated slag by using combined embedded ultrasonic measurement, thermal analysis, XRD, FTIR and SEM", *Composites Part B: Engineering*, vol. 186, art. no. 107840, 2020, doi: [10.1016/j.compositesb.2020.107840](https://doi.org/10.1016/j.compositesb.2020.107840).
- [8] L. Li, D. Xu, S. Huang, and X. Cheng, "Investigation of piezoelectric composite transducer in Ultrasonic monitoring of cement hydration", *Advances in Cement Research*, vol. 27, no. 7, pp. 424–432, 2015, doi: [10.1680/adcr.14.00032](https://doi.org/10.1680/adcr.14.00032).
- [9] S.K. Nath and S. Kumar, "Reaction kinetics of fly ash geopolymerization: Role of particle size controlled by using ball mill", *Advanced Powder Technology*, vol. 30, no. 5, pp. 1079–1088, 2019, doi: [10.1016/j.appt.2019.03.003](https://doi.org/10.1016/j.appt.2019.03.003).
- [10] Z. Zhang, J.L. Provis, H. Wang, F. Bullen, and A. Reid, "Quantitative kinetic and structural analysis of geopolymers. Part 2. Thermodynamics of sodium silicate activation of metakaolin", *Thermochimica Acta*, vol. 565, pp. 163–171, 2013, doi: [10.1016/j.tca.2013.01.040](https://doi.org/10.1016/j.tca.2013.01.040).
- [11] K.I. Ku Marsilla and C.J.R. Verbeek, "Crystallization of itaconic anhydride grafted poly(lactic acid) during annealing", *Journal of Applied Polymer Science*, vol. 134, no. 12, pp. 1–11, 2017, doi: [10.1002/app.44614](https://doi.org/10.1002/app.44614).
- [12] J. Fournier, "Application of the JMAK model for crystal dissolution kinetics in a borosilicate melt", *Journal of Non-Crystalline Solids*, vol. 489, pp. 77–83, 2018, doi: [10.1016/j.jnoncrysol.2018.03.018](https://doi.org/10.1016/j.jnoncrysol.2018.03.018).
- [13] J. Torrens-Serra, S. Venkataraman, M. Stoica, U. Kuehn, S. Roth, and J. Eckert, "Non-isothermal kinetic analysis of the crystallization of metallic glasses using the master curve method", *Materials (Basel)*, vol. 4, no. 12, pp. 2231–2243, 2011, doi: [10.3390/ma4122231](https://doi.org/10.3390/ma4122231).
- [14] A.A. Siyal, K.A. Azizli, Z. Man, L. Ismail, and M.I. Khan, "Geopolymerization kinetics of fly ash based geopolymers using JMAK model", *Ceramics International*, vol. 42, no. 14, pp. 15575–15584, 2016, doi: [10.1016/j.ceramint.2016.07.006](https://doi.org/10.1016/j.ceramint.2016.07.006).
- [15] A.H. Pauzi, L. Ismail, A.A. Siyal, Z. Man, and K.A. Azizli, "Experimental study of geopolymer solidification kinetics", *Applied Mechanics and Materials*, vol. 625, pp. 127–130, 2014, doi: [10.4028/www.scientific.net/AMM.625.127](https://doi.org/10.4028/www.scientific.net/AMM.625.127).

- [16] ASTM Committee C09.48, ASTM C1679-14 Standard Practice for Measuring Hydration Kinetics of Hydraulic Cementitious Mixtures Using Isothermal Calorimetry. ASTM, 2014, doi: [10.1520/C1679-14.2](https://doi.org/10.1520/C1679-14.2).
- [17] “Standard Test Method for Measurement of Heat of Hydration of Hydraulic Cementitious Materials Using Isothermal Conduction”. ASTM, 2014, doi: [10.1520/C1702-09a.2](https://doi.org/10.1520/C1702-09a.2).
- [18] G. De Schutter and L. Taerwe, “General hydration model for portland cement and blast furnace slag cement”, *Cement and Concrete Research*, vol. 25, no. 3, pp. 593–604, 1995, doi: [10.1016/0008-8846\(95\)00048-H](https://doi.org/10.1016/0008-8846(95)00048-H).
- [19] A. Rafeet, R. Vinai, M. Soutsos, and W. Sha, “Effects of slag substitution on physical and mechanical properties of fly ash-based alkali activated binders (AABs)”, *Cement and Concrete Research*, vol. 122, pp. 118–135, 2019, doi: [10.1016/j.cemconres.2019.05.003](https://doi.org/10.1016/j.cemconres.2019.05.003).
- [20] R. Cornelis, H. Priyosulistyo, and I. Satyarno, “The Investigation on Setting Time and Strength of High Calcium Fly Ash Based Geopolymer”, *Applied Mechanics and Materials*, vol. 881, pp. 158–164, 2018, doi: [10.4028/www.scientific.net/AMM.881.158](https://doi.org/10.4028/www.scientific.net/AMM.881.158).

Received: 2023-10-29, Revised: 2024-01-30